

AD627231

TR 66-3

**ADVANCEMENT OF ULTRASONIC
TECHNIQUES USING RERADIATED SOUND
ENERGIES FOR NONDESTRUCTIVE
EVALUATION OF WELDMENTS**

January 15, 1966

CLEARINGHOUSE
FOR FEDERAL SCIENTIFIC AND
TECHNICAL INFORMATION

Hardcopy

Microfilm

\$ 1.00

\$ 0.50

22

as

ARCHIVE COPY

Code 1



Automation Industries, Inc.

RESEARCH DIVISION - BOULDER, COLORADO

Quarterly Progress Report No. 2

**ADVANCEMENT OF ULTRASONIC TECHNIQUES
USING RERADIATED SOUND ENERGIES FOR
NONDESTRUCTIVE EVALUATION OF WELDMENTS**

**B. T. Cross
G. L. Cross
G. J. Posakony**

**Automation Industries, Inc.
Research Division
Boulder, Colorado 80302**

**Contract No. NObs - 92530
Serial No. SR007-10-04, Task No. 891**

January 15, 1966

**Chief, Bureau of Ships, Code 634B
Department of the Navy
Washington, D. C.**

FOREWORD

This second quarterly progress report was prepared by Automation Industries, Inc., Research Division, under Bureau of Ships Contract NObs 92530. This project was initiated to conduct a feasibility study to determine the physics of reradiated sound energy and to determine the practicability of using reradiated sound energy rather than reflected sound energy as a weld inspection tool. Mr. D. L. Keaton is acting as the Bureau of Ships Project Engineer. The work is being performed under Project Serial No. SR007-10-04, Task No. 891.

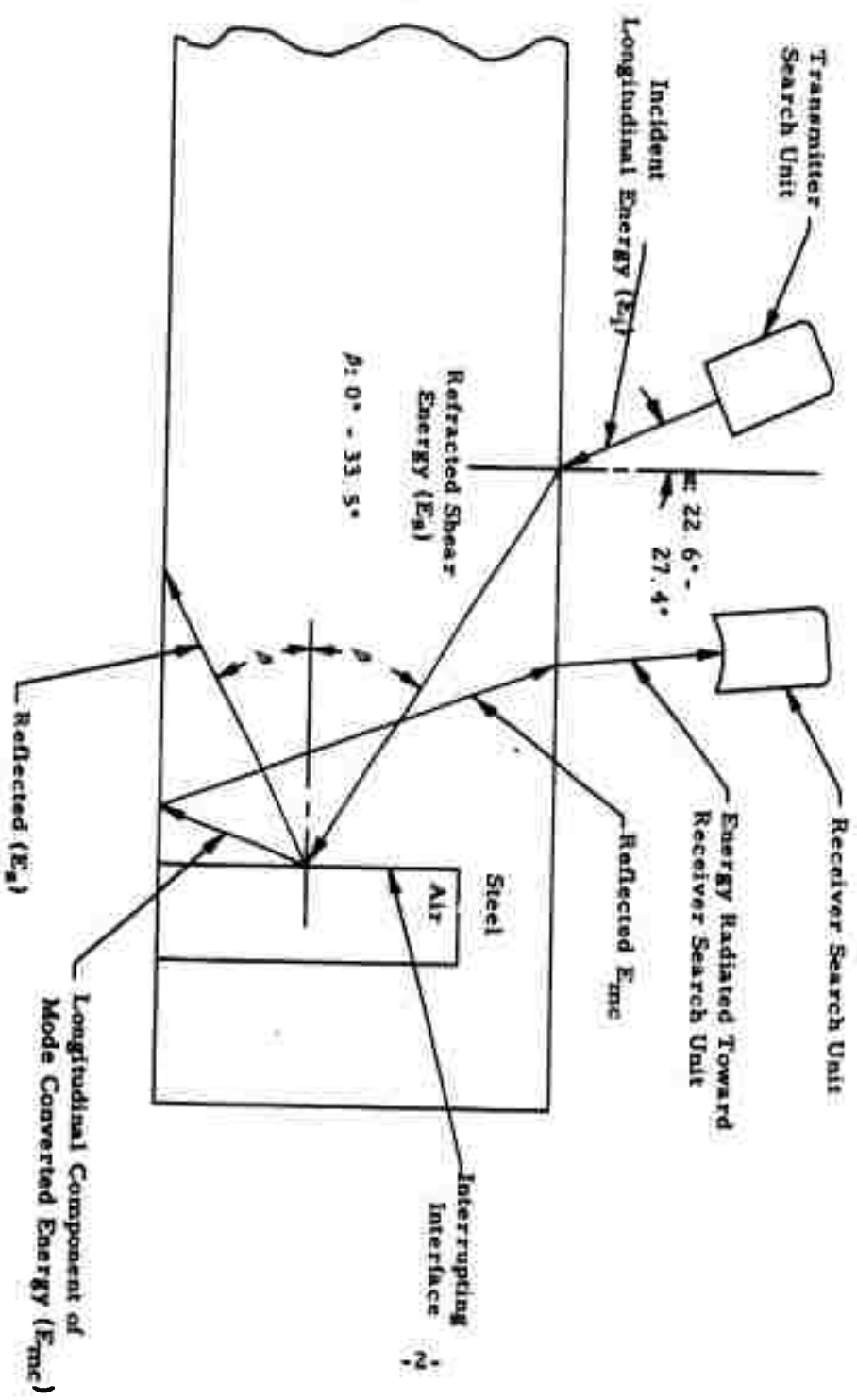
The period of work covered by this report is from 1 October 1965 to 31 December 1965. Previous work was reported in Quarterly Progress Report No. 1, TR 65-75, November 15, 1965.

SUMMARY

The long range objective of the work being performed under this contract is to find a better technique for ultrasonic nondestructive evaluation of weldments. The immediate objective is to provide a clearer understanding of the ultrasonic weld inspection technique known as the "Delta Configuration". This technique has been employed for several years, but the approach has been entirely empirical. Work reported in AFML-TR 65-84 shows an encouraging potential for the approach. Before further advances could be made, analytical verification of the physics of the sound energy had to be established. Once the path and pattern of the sound energy can be predicted, instrumentation and fixturing can be developed which will amplify the merits of this technique.

In the first report prepared under this contract, Progress Report No. 1 dated 15 November 1965, an extensive literature survey was reported which was applicable to the subject of the contract. In addition, the initial analysis of the physics of the reradiated sound energy was presented.

In this second report, the analysis made in Progress Report No. 1 is verified empirically. A test block, designed to study the phenomena, was used to obtain field intensity maps of the sound energy. The tests provided an unexpected result in that a second energy conversion was identified. The existence of this second mode conversion was verified by using the same mathematical procedure used in Progress Report No. 1. Knowledge obtained is important because it increases the potential of using the Delta Configuration for both thick and thin weldments.



Predicted Sound Energy Paths Used in "Delta Configuration"

I. INTRODUCTION

1.0 Summary of Progress Report No. 1

The advantage of the Delta Configuration technique as employed in ultrasonic nondestructive testing is that defects of random orientation can be detected and evaluated. Other ultrasonic testing techniques have a limitation because of their inherent sensitivity to defect orientation. The initial analysis performed in the first progress report provided some of the basis for a better understanding of the reasons why the Delta technique is relatively insensitive to the orientation of the defect.

Empirical results show the desired location for the two ultrasonic search units used in this technique. An analysis was performed which showed the sound energy paths needed to fulfill the requirements. Figure 1 shows the predicted sound paths for Delta operation. The angular ranges indicated in Figure 1 were calculated to satisfy the requirements for steel. Briefly, the results obtained were as follows:

- A. An incident longitudinal wave transmitted in water must impinge on the part surface in a specific angular region. The angular region is determined by the restrictions imposed by Item 'C'.
- B. The resultant shear wave in the metal must propagate toward the weld zone at angle β . The angle β is controlled by the incident angle α ; however, β must satisfy conditions in Item C.
- C. A mode conversion must occur at the interrupting interface. This mode conversion will only occur for a discrete range of angle β , dependent on the longitudinal and shear velocities of the material.
- D. The longitudinal energy component of the mode conversion must be reflected from the bottom surface and then radiated from the top surface toward the receiver search unit.
- E. To achieve a mode conversion, the interrupting interface need not lie at a specific angle.
- F. The energy received at the receiving search unit can be mode converted energy or direct radiated energy depending on the configuration of the interface.

II. WORK PERFORMED FOR THIS PERIOD

1.0 Introduction

The purpose of the work performed during the second work period was threefold: (a) to empirically establish validity of the analysis made in Progress Report No. 1, (b) to measure any deviation from the predicted pattern of wave behavior, and (c) if a deviation exists, to mathematically verify and define that wave behavior.

2.0 Validity of Analysis in Progress Report No. 1

Verification of the initial analysis was made by conducting ultrasonic tests under identical physical conditions. The sound energy path predictions were based on two restricting physical conditions: (a) the material being tested was steel, and (b) the interrupting interface was a solid-to-air interface. A test sample was fabricated from a low alloy steel to satisfy the material condition. A rectangular cavity was machined in the sample and sealed to satisfy and maintain the interface condition. See Figure 2.

The ultrasonic test method was to project sound energy into the sample and to measure the field intensity and location of the reradiated sound energy.

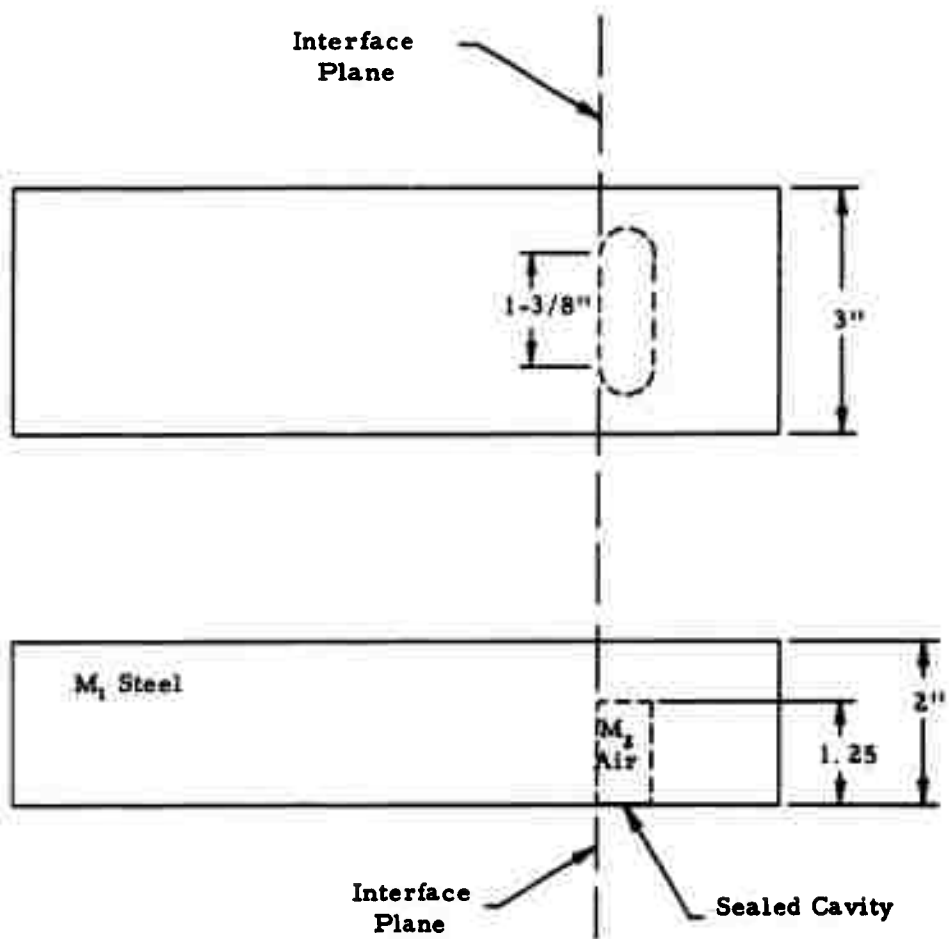
3.0 Detection of Unpredicted Wave Behavior

All ultrasonic fields radiating from the top surface of the sample, in the vicinity of the interrupting interface, were recorded and mapped as to location, intensity, and time of travel. The results of these tests were compared to predicted wave patterns. Any deviation from the predicted pattern will be analyzed and defined mathematically.

4.0 Test Procedure

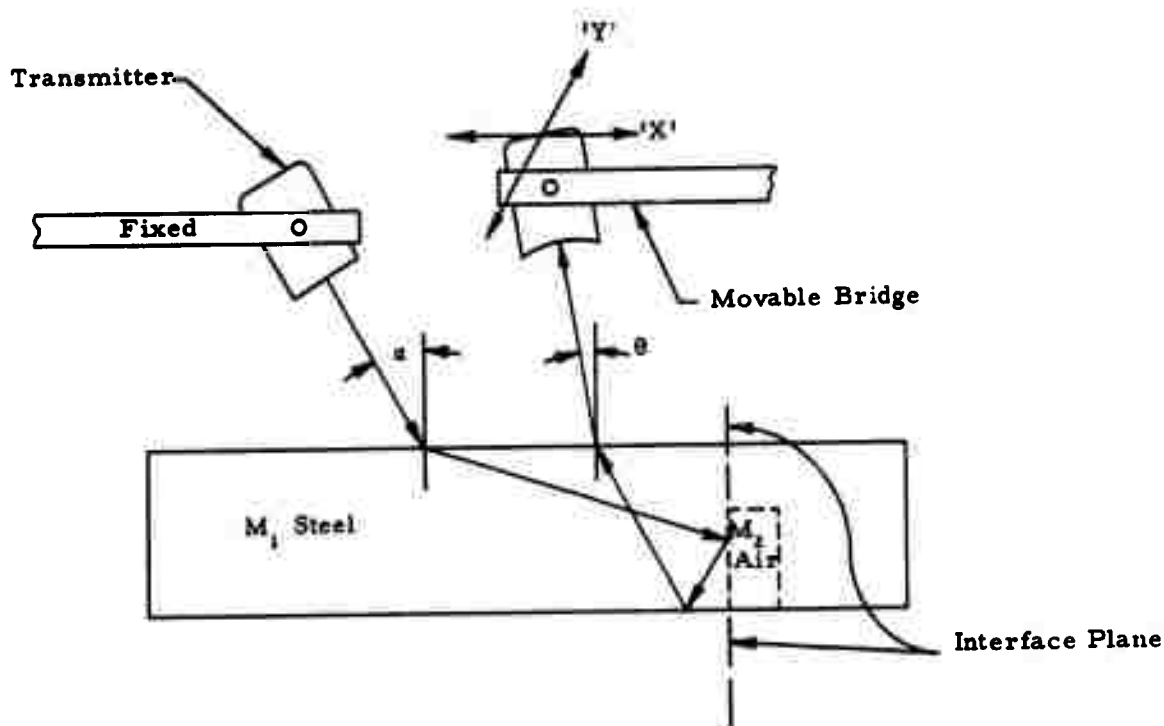
The same test procedure was used for all study performed during this period. The procedure was to transmit sound energy from a stationary search unit in a pre-aligned position and to receive the redirected energy with another search unit positioned by a movable bridge. Figure 3 shows the search unit configuration and the directions of bridge movement.

A 5.0 MHz., 0.375" diameter transmitter search unit was used to keep the beam diameter small. This restricted the energy from overlapping



Test Sample No. 1

Figure No. 2



"Delta Configuration" Used for Mapping Field Intensity

Figure No. 3

the interface and causing reflections beyond the interface which might be interpreted as deviations from the predicted behavior. The receiver search unit was required to discriminate between the radiated ultrasonic energy and the reflected surface energy, while sampling small increments of the radiated field. A 5.0 MHz, 0.25" diameter search unit with a focused lens was used for the receiver. The small search unit allows a point by point sampling of the field pattern.

The field intensity data was recorded as 'received signal' amplitude with a Houston Instruments 'X-Y' Recorder, Model HR-97. The 'receiver' search unit position was referenced to the recorder by (a) a data potentiometer attached to the bridge for 'X' direction information, and (b) a predetermined 'Y' direction index of the recorder pen corresponding to a 1/16" receiver index in the 'Y' direction. The 'received signal' amplitude was isolated by electronic 'gating' circuits and fed directly into the recorder 'Y' amplifier. The amplitude information was recorded as an excursion from the 'Y' position reference line.

Field plots were made at transmitter incident angles of 23.0°, 23.5°, 24.5°, and 25.5°. The data was recorded and plotted as signal amplitude; however, signal amplitude is directly related to acoustical pressure striking the receiver search unit. The lines shown in the field plots are equal pressure points which indicate the intensity of the acoustical energy at the surface of the part.

The 'receiver' amplifier gain was adjusted to 90% FSD (full scale deflection) for the peak 'received signal' with a transmitter angle $\alpha = 23.0^\circ$. This gain level was kept constant for all tests. Each test results in a field map. The 'receiver' search unit was tilted to a predetermined angle for each prescribed transmitter incident angle. This allowed the 'receiver' search unit to be more normal to the radiating energy.

5.0 Test Results

The field plots are shown in Figures No. 4, 5, 6, 7, 8, 9, and 10.

The field plots shown in Figures No. 4, 5, 7, and 9 are the fields resulting from wave E_{mcr} . Figures No. 6, 8, and 10 are fields resulting from wave E_{mcs} .

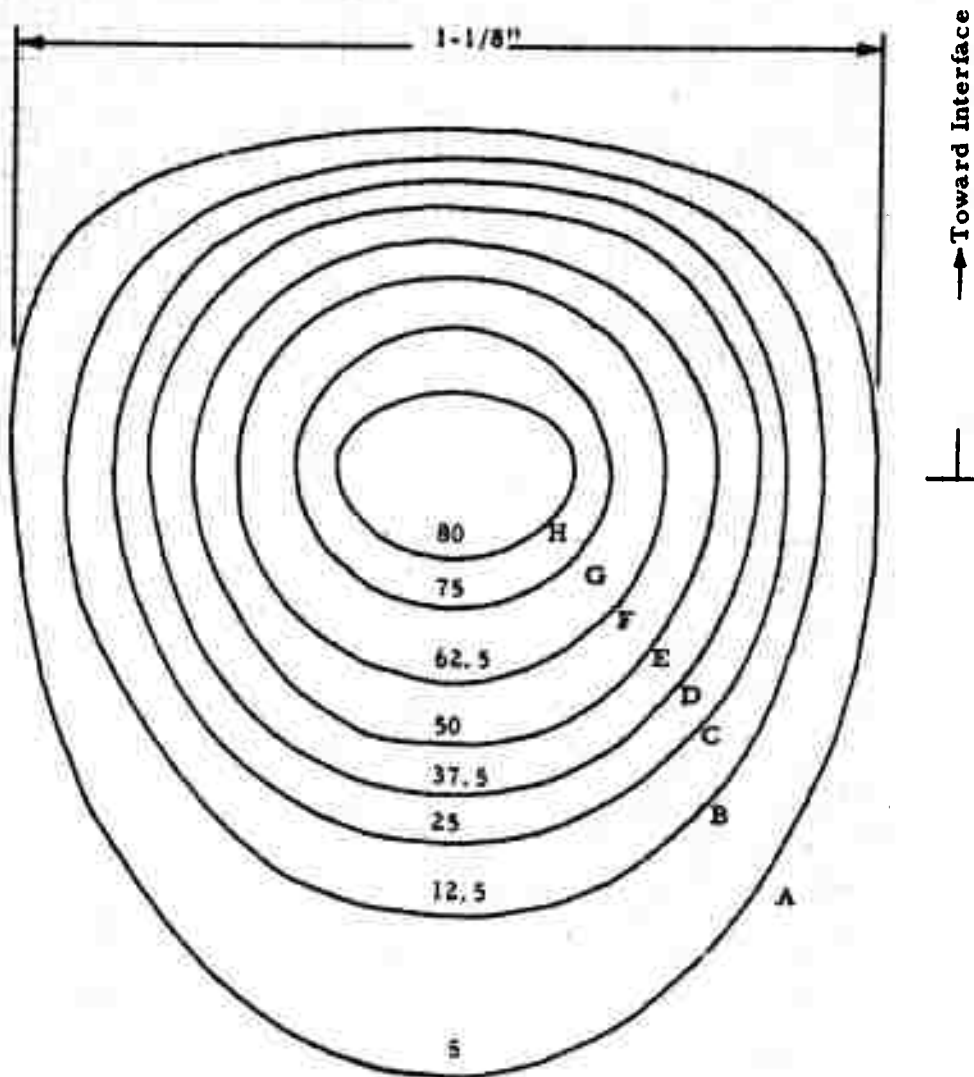
A detailed explanation of the field plots is shown in the following discussion of Figure No. 4. The field map shown was made for a transmitter angle α equal to 23°. The map consists of a series of closed lines called equal pressure lines. The equal pressure line means: (a) the acoustical pressure directly above that line caused a receiver signal amplitude of the

Numbers on field lines
are % FSD.

The measured distance from
the center of the field to the
interface plane is $9/16"$.

Scale:

3 div. = $1/16"$



Radiation Field for E_{mcr} with $\alpha = 23^\circ$

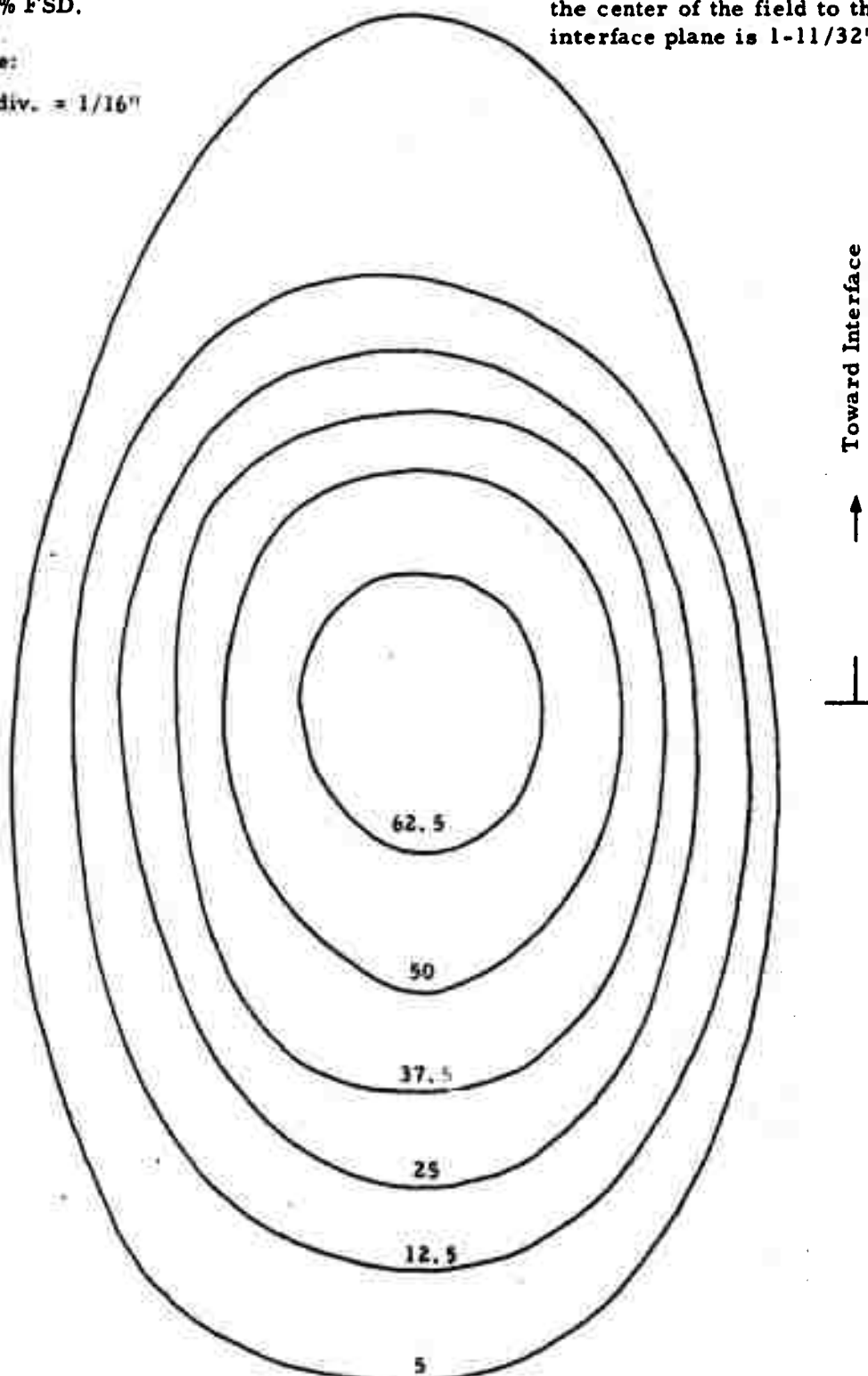
Figure No. 4

Numbers on field lines
are % FSD.

Scale:

3 div. = 1/16"

The measured distance from
the center of the field to the
interface plane is 1-11/32"



Radiation Field of E_{mcr} with $\alpha = 23.5\%$

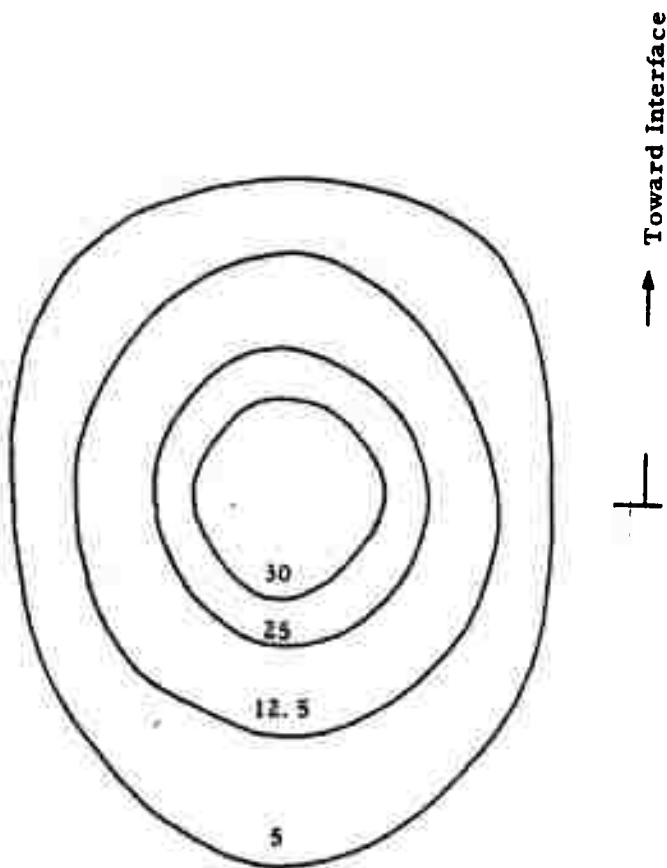
Figure No. 5

Number on field lines
are % FSD.

Scale:

3 div. = 1/16"

The measured distance from
the center of the field to the
interface plane is 1-3/32".



Radiation Field of E_{mcs} with $\alpha = 23.5^\circ$

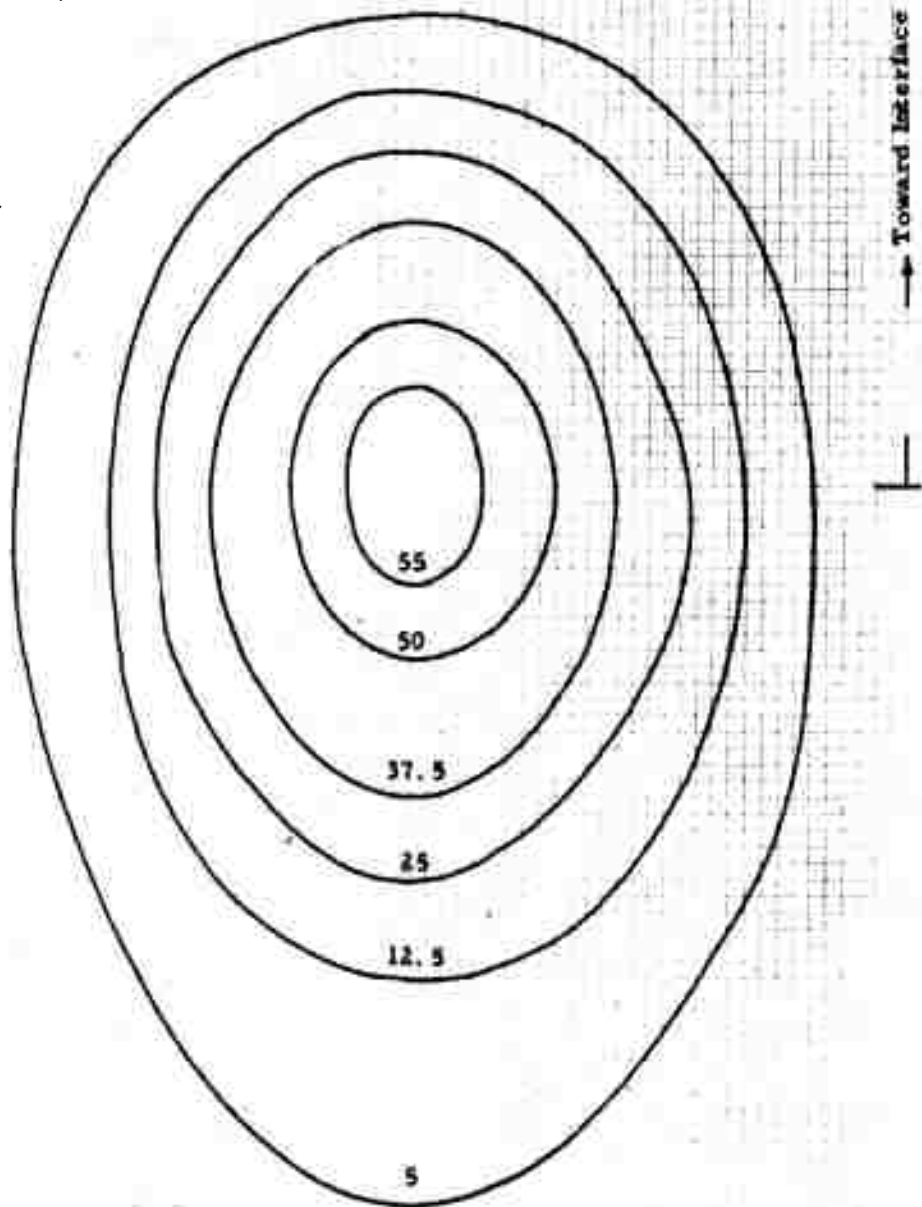
Figure No. 6

Numbers on field lines
are % FSD.

The measured distance from
the center of the field to the
interface plane is $1-7/16''$.

Scale:

3 div. = $1/16''$



Radiation Field of E_{mcr} with $\alpha = 24.5^\circ$

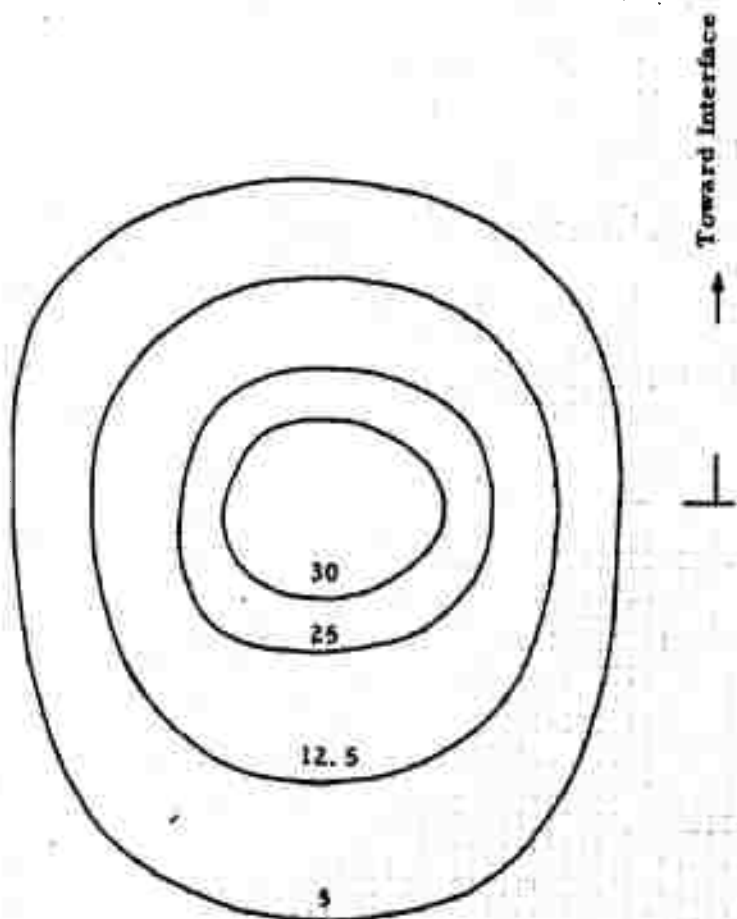
Figure No. 7

Numbers on field lines
are % FSD.

Scale:

3 div. = 1/16"

The measured distance from
the center of the field to the
interface plane is 1-1/16".



Radiation Field of E_{mcs} with $\alpha = 24.5^\circ$

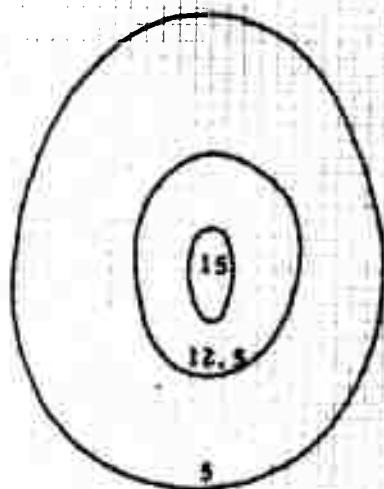
Figure No. 8

Numbers on field lines
are % FSD.

Scale:

3 div. = $1/16''$

The measured distance from
the center of the field to the
interface plane is $1-15/16''$.



Radiation Field of E_{mcv} with $\epsilon = 25.5^\circ$

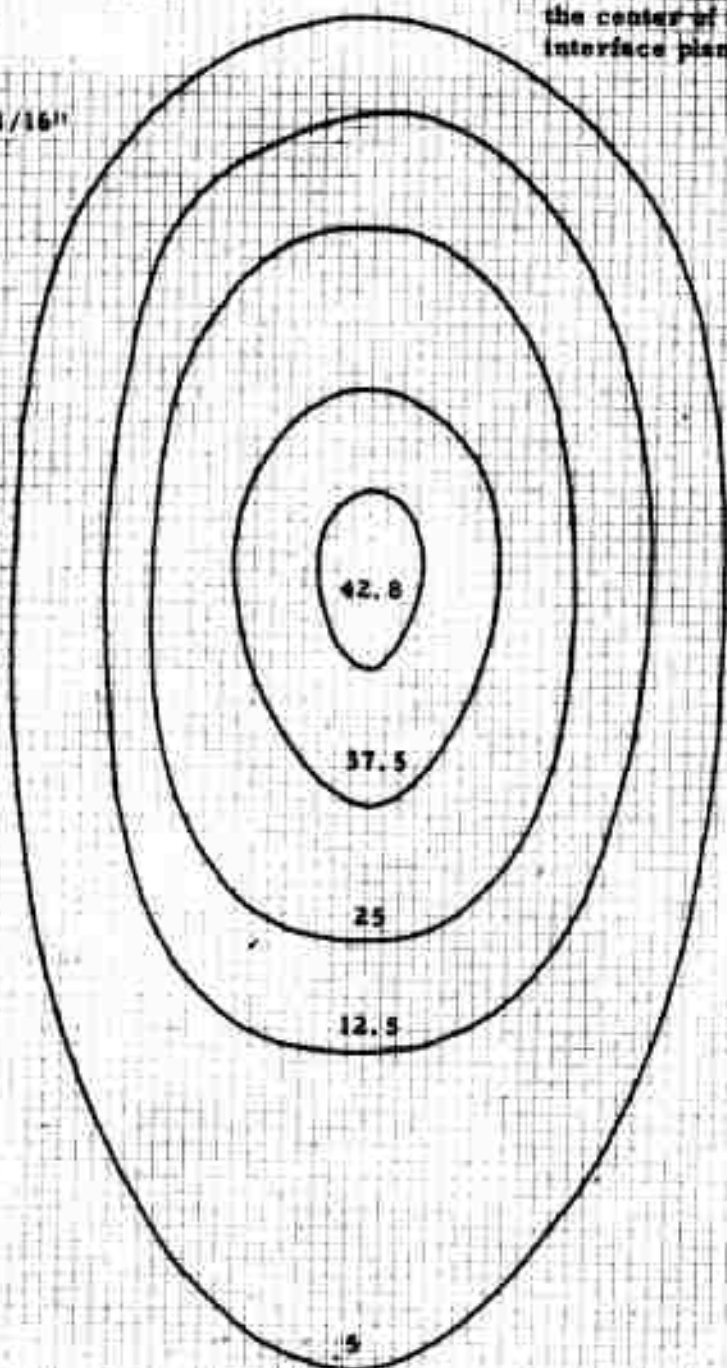
Figure No. 9

Numbers on field lines
are % FSD.

Scale:

3 div. = 1/16"

The measured distance from
the center of the field to the
interface plane is 1-3/8".



Radiation Field of E_{mc} with $\epsilon = 25.5^\circ$

Figure No. 10

designated value, (b) the acoustical pressure outside that line was lower and caused a receiver signal of lower amplitude, and (c) the acoustical pressure inside that line was greater and caused a receiver signal of greater amplitude. For example, equal pressure line E represents the measured location of acoustical pressure that caused a receiver signal amplitude of 50% FSD. The acoustical pressure at 'F' caused a signal amplitude of 62.5%. The measured distance from the center of the field map to the interface plane is noted at the top of each figure.

The field plots in Figures No. 5 and 6 are for transmitter angle $\alpha = 23.5^\circ$. Two distinct fields of radiating energy are shown for the transmitter angle α equal to 23.5° . The two field phenomena was observed for angle α equal to 24.0° and 25.5° , Figures No. 7-8 and 9-10, respectively.

5.1 Discussion of Test Results

Multiple reflections were observed in earlier work with the "Delta Configuration"; however, these reflections were considered as multiple reflections of the mode converted wave E_{mc} . A detailed study of the transmission time and the physical location on the surface revealed that neither agreed with the 'multiple' concept. It had been assumed that the energy radiating from the top surface was caused by the reflected wave E_{mcr} . See Figure No. 11. The presence of two distinctive waves at the top surface established the existence of a second wave propagating from the bottom surface toward top surface. The initial analysis in Progress Report No. 1 mathematically verified existence of E_{sr} (reflected shear) and E_{mc} (mode converted longitudinal) radiating from the interrupting interface. See Figure No. 11.

The ray analogy used in Figure No. 11 shows the wave behavior at the bottom surface. A second mode conversion occurs when wave E_{mc} impinges on the bottom surface. The initial analytical analysis defined the range of energy incidence which allowed mode converted wave E_{mc} to exist (the range of α was from 22.6° to 27.4°). Referring to Figure No. 11, if we maintain the incident energy at α within the specified angles, the resultant energy E_{mc} will fall within the limit of γ ($11^\circ \leq \gamma \leq 72^\circ$). Snell's law verifies the existence of waves E_{mcr} and E_{mcs} , and defines the limits of angle ϕ . For α within the specified range, ϕ will lie between $6^\circ \leq \phi \leq 31.5^\circ$. The same mathematical analysis used in Progress Report No. 1 was used to verify and define the second mode conversion.

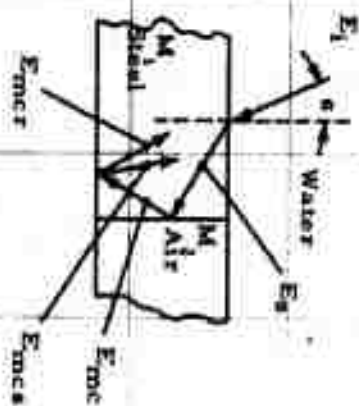
The formulae from Ergin's¹⁵ paper were used to quantitatively analyze the partition of energy in the second mode conversion. Figure No. 12 shows the energy ratios of the various wave components in the region of interest. The transferral of energy from wave E_{mcr} to wave E_{mcs}

Calculated Energy
Incident Energy

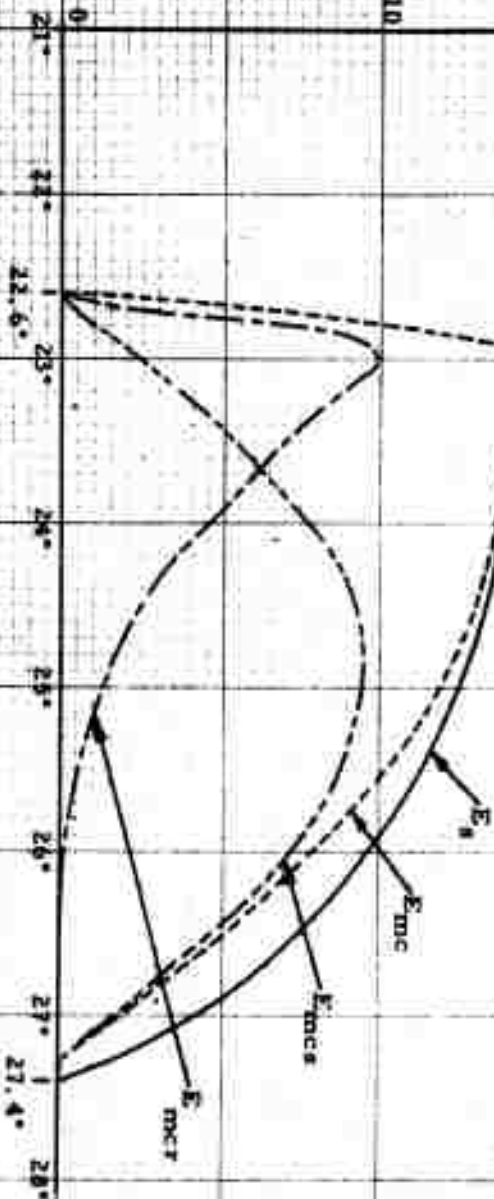
Energy Ratio

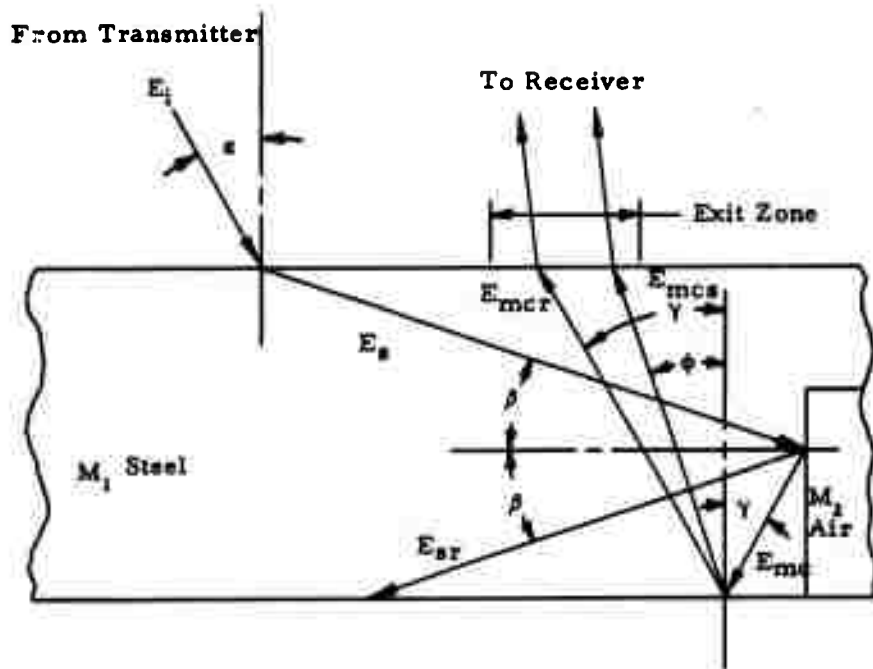
0.25
0.20
0.10
0

E_s
 E_{mc}
 E_{mcr}
 E_{mcs}



Angle of Incidence of Longitudinal Energy E_i
Energy Partition at First and Second Mode Conversions





Ray Analogy of "Delta Configuration"

Figure No. 11

as the angle α increases, will tend to hold the exit zone* in proximity of the interrupting interface. Energy reception is enhanced by the integration of the energies E_{mcs} and E_{mcr} .

6.0 Conclusions Reached During Second Work Period

The analytical analysis of the "Delta Configuration" concept has been expanded by the second mode conversion. Reiterating briefly, the latest "Delta" analysis is the following: (See Figure No. 11)

- (1) A longitudinal wave E_i propagating in water is incident upon the top surface of a part (M_1) at angle α , causing a refracted shear wave E_s to propagate in the part (M_1 steel) at some angle $90^\circ - \beta$.
- (2) The shear wave E_s impinges on the interrupting interface (steel-to-air) at angle β . Angle β is dependent upon angle α , longitudinal velocity in water, and the shear velocity in M_1 .
- (3) The shear wave E_s is reflected by the interface at angle β and if angle β lies within certain limits, a mode conversion causes a longitudinal wave E_{mc} to be radiated at angle γ from the interface.
- (4) The radiated longitudinal wave E_{mc} strikes the bottom surface causing a second mode conversion.
- (5) The second mode conversion splits longitudinal wave E_{mc} into waves E_{mcr} (reflected E_{mc}) and E_{mcs} (mode converted shear wave) which propagates towards the top surface.
- (6) Waves E_{mcr} and E_{mcs} , upon striking the top surface, are refracted and propagate in the water as longitudinal energy. This energy is detected by the "Delta Configuration" 'receiver' search unit.

The ray analogy in Figure No. 11 illustrates why energy is received with the "Delta Configuration" near the interrupting interface plane and why no signal is received unless an interrupting interface exists.

*The exit zone is defined as the region where the ultrasonic energy reradiates from the top surface.

IV. PROGRAM FOR NEXT PERIOD

The work program for the third quarter includes:

- (1) A study of the effects caused by reducing the cross-sectional area of the interrupting interface and by varying its shape and orientation.**
- (2) A study of search unit size, material, and frequency combinations applied in the "Delta Configuration".**
- (3) Selection and initial "Delta" inspection of weld samples to be used.**
- (4) A series of tests utilizing oscillating transmitter and receiver search units in the "Delta Configuration".**
- (5) An empirical analysis conducted with the Schlieren System.**